

**Electronic Supporting Information for**

**Interstratified heterostructures of metal hydroxide  
nanoclusters and MoS<sub>2</sub> monolayers with improved  
electrode performance**

Tae-Ha Gu,<sup>§a</sup> Jungeun Kim,<sup>§a</sup> Seung Mi Oh,<sup>a</sup> Xiaoyan Jin,<sup>b</sup> and Seong-Ju Hwang<sup>\*b</sup>

<sup>a</sup> Department of Chemistry and Nanoscience, College of Natural Sciences, Ewha Womans  
University, Seoul 03760, Korea

<sup>b</sup> Department of Materials Science and Engineering, College of Engineering, Yonsei University,  
Seoul 03722, Korea

**Fig. S1.** Energy dispersive spectrometry (EDS)–elemental maps of (a) CrMS1 and (b) CrMS2.

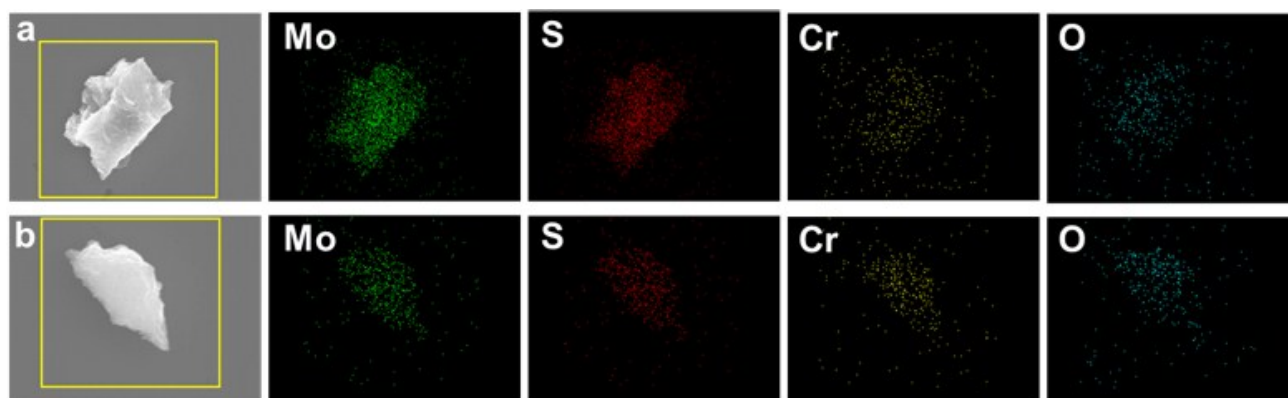


**Fig. S2.** O 1s X-ray photoelectron spectra for CrMS nanohybrids.

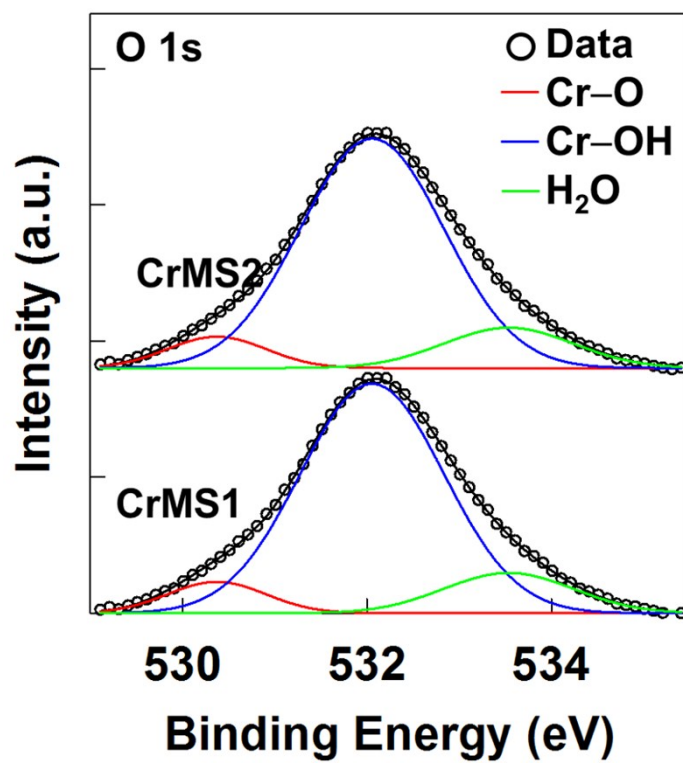


**Fig. S3.** Structural models for pillared chromium hydroxide nanoclusters.

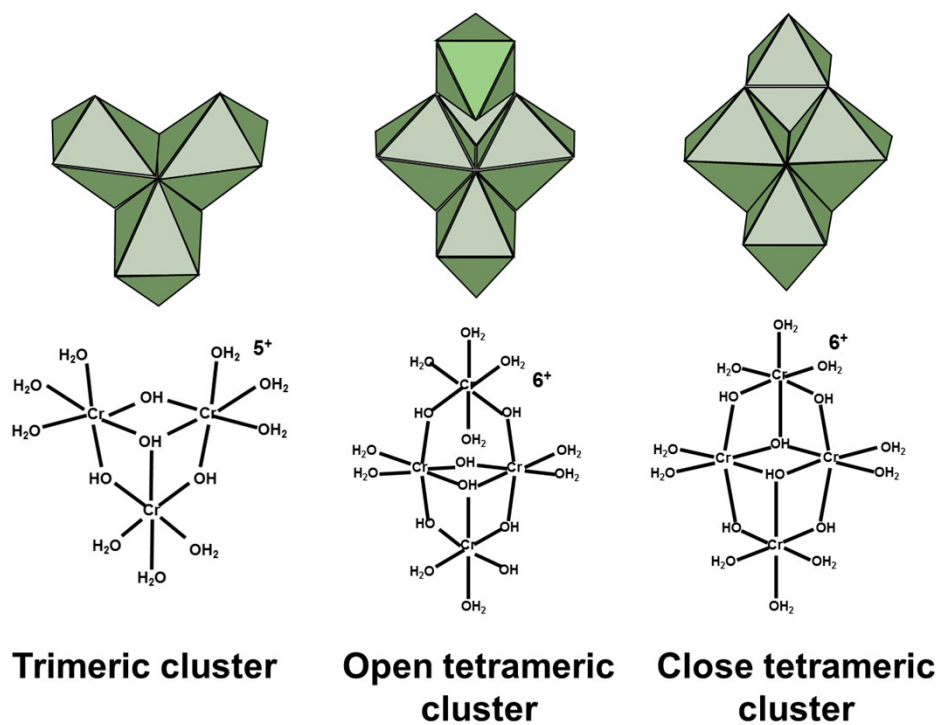


**Fig. S4.** Fourier transformed (left) and Fourier-filtered (right) spectra of Cr K-edge extended X-ray absorption fine structure (EXAFS) data for **CrMS2** with (a) trimeric, (b) open tetrameric, and (c) closed tetrameric structure models. Among the present models, the open tetrameric model gives the best fits to the experimental data, as highlighted in the red box.

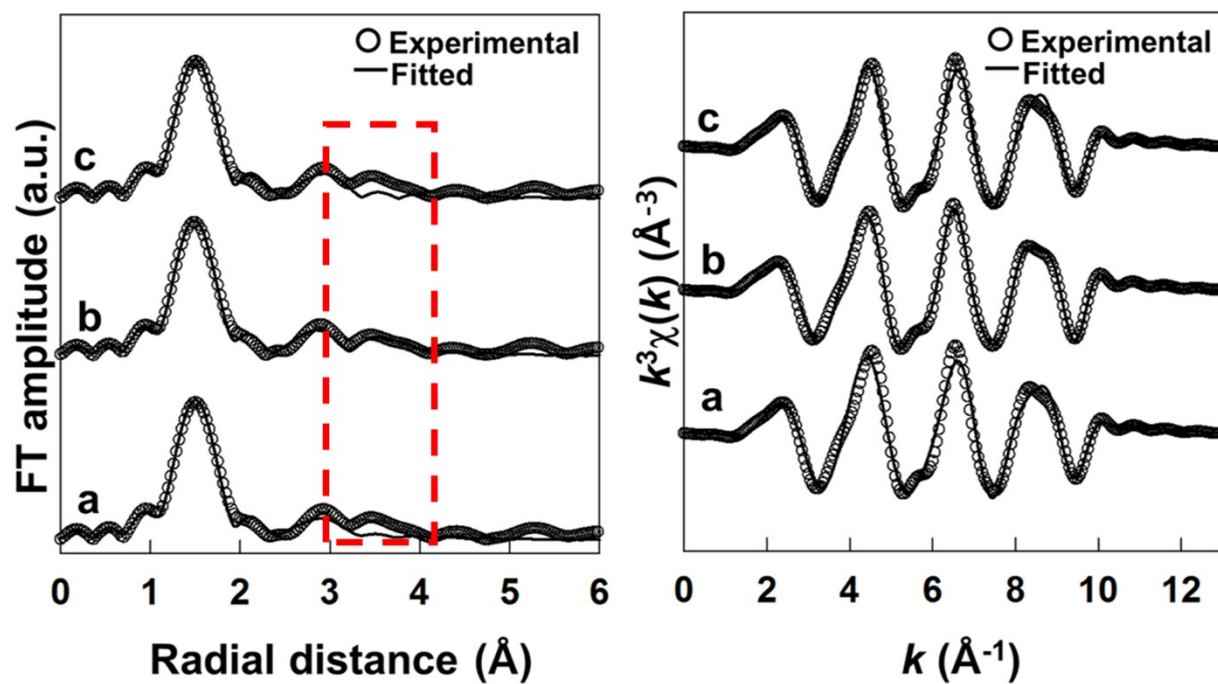


**Fig. S5.** Differential capacity vs. voltage ( $dQ/dV$ ) curves for (a) bulk  $\text{MoS}_2$ , (b) **CrMS1**, and (c) **CrMS2**.

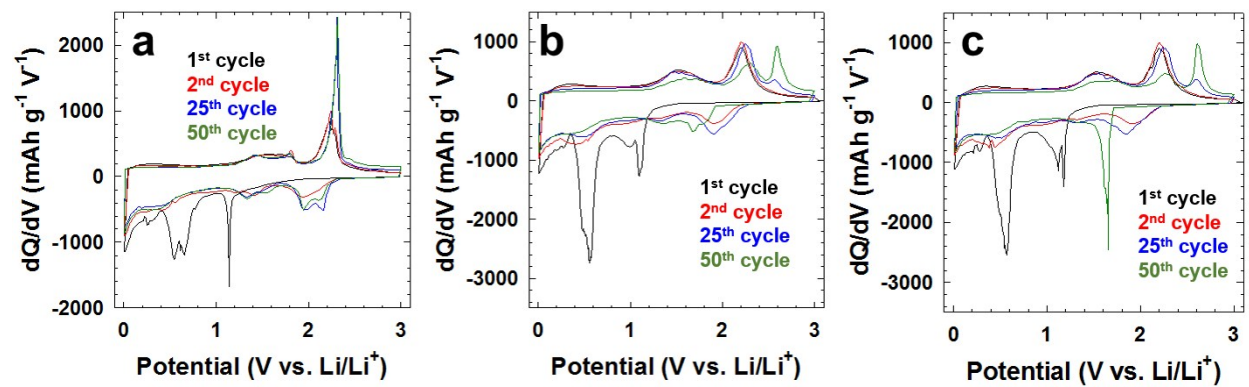


**Table S1.** Relative concentration of oxygen species for **CrMS** nanohybrids.

Materials	Cr–O	Cr–OH	H <sub>2</sub> O
<b>CrMS1</b>	8.8 %	82.9 %	8.3 %
<b>CrMS2</b>	7.5 %	79.9 %	12.6 %

**Table S2.** Parameters obtained by fitting analyses for Nyquist plots on the basis of the Voigt-type equivalent circuit.

Materials	$R_s$ ( $\Omega$ )	$R_{ct}$ ( $\Omega$ )
Bulk MoS <sub>2</sub>	24.73	157.0
<b>CrMS1</b>	20.08	143.4
<b>CrMS2</b>	24.67	136.2